

Published in final edited form as:

Biochem Biophys Res Commun. 2010 January 1; 391(1): 443–448. doi:10.1016/j.bbrc.2009.11.077.

GTPase activating protein function of p85 facilitates uptake and recycling of the $\beta 1$ integrin

Traci E. Stankiewicz, Kelsey L. Haaning, Janelle M. Owens, Alys S. Jordan, Kelly Gammon, Heather A. Bruns, and Susan A. McDowell

Ball State University, Muncie, IN, USA

Abstract

$\beta 1$ -containing adhesions at the plasma membrane function as dynamic complexes to provide bidirectional communication between the cell and its environment, yet commonly are used by pathogens to gain host cell entry. Recently, the cholesterol lowering drug simvastatin was found to inhibit host invasion through $\beta 1$ -containing adhesion complexes. To better understand the regulatory mechanisms controlling adhesion formation and uptake and the use of these complexes by *Staphylococcus aureus*, the primary etiologic agent in sepsis, bacteremia and endocarditis, we investigated the mechanism of inhibition by simvastatin. In response to simvastatin, adhesion complexes diminished as well as $\beta 1$ trafficking to the plasma membrane required to initiate adhesion formation. Simvastatin stimulated CDC42 activation and coupling to p85, a small-guanosine triphosphatase (GTPase) activating protein (GAP), yet sequestered CDC42 coupled to p85 within the cytosol. Loss of p85 GAP activity through use of genetic strategies decreased host cell invasion as well as $\beta 1$ trafficking. From these findings, we propose a mechanism whereby p85 GAP activity localized within membrane compartments facilitates $\beta 1$ trafficking. By sequestering p85 within the cytosol, simvastatin restricts the availability and uptake of the receptor used by pathogenic strains to gain host cell entry.

Keywords

phosphoinositide 3-kinase; p85; *S. aureus*; statins; breakpoint cluster region

Introduction

The formation of adhesion complexes begins with the recruitment of $\beta 1$ from the recycling endosome to the plasma membrane [1,2]. Once localized within the plasma membrane, $\beta 1$ functions as an anchor for the ordered assemblage of components into the complex [3]. These complexes then provide bidirectional communication between the cell and its environment as well as a route of access for pathogenic strains of *S. aureus* [4]. Invasion is facilitated by fibronectin, a ligand of $\alpha 5\beta 1$, that avidly binds to fibronectin-binding proteins expressed on the bacterial cell wall. When fibronectin-bound *S. aureus* engages $\alpha 5\beta 1$, bacteria are internalized with the ligand/receptor complex. Although originally described as an

© 2009 Elsevier Inc. All rights reserved.

Request reprints from: Susan A. McDowell, Ph.D., Cooper Science Complex, CL 171C, 2111 Riverside Ave., Ball State University, Muncie, IN 47306, Phone: +1-765-285-8846, FAX: +1-765-285-8804, samcdowell@bsu.edu.

Publisher's Disclaimer: This is a PDF file of an unedited manuscript that has been accepted for publication. As a service to our customers we are providing this early version of the manuscript. The manuscript will undergo copyediting, typesetting, and review of the resulting proof before it is published in its final citable form. Please note that during the production process errors may be discovered which could affect the content, and all legal disclaimers that apply to the journal pertain.

extracellular pathogen, an emerging concept is that internalized *S. aureus* can evade host immune responses, extracellular antibiotic therapy and the phago/lysosomal pathway, to initiate recurrent, often severe, infection [5].

Simvastatin inhibits this internalization [6]. This inhibition of invasion may contribute to protective effects in individuals on a statin regimen for hypercholesterolemia, including improved cardiac output [7] and immunomodulatory effects, that are associated with a decreased risk of death due to bacteremia or sepsis [8–10]. The mechanism of action of statins is competitive inhibition of 3-hydroxy-3-methylglutaryl coenzyme A (HMG-CoA) reductase at an early step in the cholesterol biosynthesis pathway [11]. Inhibition at this early step decreases plasma levels of cholesterol as well as intermediates within the cholesterol biosynthesis pathway. Intermediates include the isoprenoids farnesyl and geranylgeranyl pyrophosphate, long, hydrophobic groups that function as membrane anchors and facilitate protein-protein interactions of target proteins [12]. Proteins are targeted for prenylation by a conserved CaaX motif. The depletion of isoprenoids by statins diminishes post-translational prenylation of target proteins and leads to pleiotropic effects that are independent of cholesterol-lowering. Inhibition of host cell invasion by simvastatin is reversed by replenishment with either farnesyl or geranylgeranyl pyrophosphate but not by replenishment with cholesterol, indicating that the mechanism includes depletion of isoprenoid intermediates [6].

This depletion of isoprenoid intermediates decreases the membrane localization of CDC42 [6], a CaaX-containing protein. Membrane localization of CDC42 is central to *S. aureus* invasion as Secramine A, an antagonist of CDC42 membrane insertion or genetic ablation of the CaaX motif are sufficient to inhibit invasion. Coupled to CDC42 through the breakpoint cluster region (BCR) homology domain, p85 accumulates within the cytosol as well. Recently, p85 was found to possess GAP activity toward a subset of small-GTPases, including CDC42 [13]. GAP proteins inactivate the GTP-bound form of their cognate small-GTPases by catalyzing the hydrolysis of GTP to GDP. As both timing and localization of this inactivation appear to be critical for appropriate trafficking of vesicles from the plasma membrane to the lysosomal or recycling compartments [14], we have investigated the hypothesis that membrane-localized p85 GAP activity facilitates β 1 trafficking and that the cytosolic sequestration of this activity by simvastatin contributes to inhibition of host invasion.

Materials and Methods

Reagents

The following were used at the concentrations and durations indicated within each figure or method described below. Simvastatin (Calbiochem, San Diego, CA); dimethyl sulfoxide (DMSO), bovine serum albumin (BSA, Fisher Scientific, Pittsburgh, PA); primaquine, tryptic soy agar, saponin, lysostaphin, gentamicin, and formaldehyde (Sigma, St. Louis, MO); FuGENE HD (Roche, Indianapolis, IN); paraformaldehyde (Electron Microscopy Sciences, Hatfield, PA), phosphate buffered saline (PBS), trypsin/EDTA, high glucose Dulbecco's Modified Eagle Medium (DMEM), Attachment Factor, M200, Low Serum Growth Supplement (LSGS), MEM Non-Essential Amino Acids, sodium pyruvate, LR Clonase (Invitrogen, Carlsbad, CA), fetal bovine serum (FBS, Atlanta Biologicals, Lawrenceville, GA), and fibronectin (MP Biomedicals, Solon, OH).

Cell culture

Human umbilical vein endothelial cells (HUVEC, Invitrogen) were cultured in M200 medium supplemented with LSGS. 3T3-Swiss albino (American Type Culture Collection, ATCC, Manassas, VA) and Human Embryonic Kidney (HEK) 293A (Invitrogen) were cultured in

DMEM supplemented with 10% FBS. U-87 MG (ATCC) were maintained in MEM supplemented with non-essential amino acids and sodium pyruvate. All cell types were maintained at 5% CO₂, 37°C, in 75 cm² vented cap flasks (Fisher).

Immunofluorescence

For confocal imaging, 3×10^4 /ml HUVEC or 3×10^2 /ml 3T3-Swiss albino were plated on 35 mm glass-bottom dishes (MatTek, Ashland, MA) coated with Attachment Factor. Treatments (detailed in results) were initiated on day 3 of plating. On day 4, cells were washed with 1X PBS, fixed (4% paraformaldehyde/PBS, 30 min), permeabilized, blocked (0.1% Triton, 1% BSA, 30 min), and incubated with anti-vinculin (Sigma-Aldrich) followed with anti-mouse Alexa Fluor 488 (Invitrogen) or stained for actin using Alexa Fluor 488 phalloidin (Invitrogen). Confocal images were acquired using an inverted Zeiss Axiovert200 microscope equipped with a plan-apochromat 40X, 1.2 NA water immersion lens with correction collar and LSM 5 Pascal scan head. Alexa 488 was excited by the 488nm Ar laser line and detected using a 505–530nm bandpass filter. Z-sectioning and frame size were set to Nyquist sampling and images generated from maximum pixel projections of Z-stacks.

β1 recycling assay

HUVEC and U-87 MG were plated at 3×10^5 /ml in 35 mm tissue culture dishes (Fisher) coated with Attachment Factor (5% CO₂, 37°C). On day 3 of plating, cells were washed extensively in 1X PBS and incubated in serum free media for 20 h (5% CO₂, 37°C). To label cell-surface β1, cells were placed at 4°C for 10 or 60 min to slow endocytosis and then incubated with anti-β1 conjugated to Alexa Fluor 488 or 555 (Invitrogen) diluted to 10 μg/ml in cold 0.01% BSA/serum free media. Following surface labeling, cells were washed twice quickly with cold 0.01% BSA in serum free media to remove unbound antibody, resuspended using cell lifters (Fisher), pelleted (1000 RPM, 5 min, 4°C), washed in cold buffer (2% BSA/PBS), fixed with cold buffer containing 0.7% formaldehyde, and analyzed using a Beckman Coulter Epics XL flow cytometer. Fluorescence indicated the population of cells with surface-labeled β1.

To examine β1 uptake and recycling, cell-surface β1 was labeled as described above. Uptake and recycling of the surface-labeled β1 was then initiated by incubating the cells at 37°C for 60 or 120 min. Following uptake/recycling, cells were subjected to two quick acid washes (0.5% glacial acetic acid/0.5 M NaCl, 3 min, 4°C on rotating platform) to remove fluorescent antibody bound to β1 that had been retained at the cell surface or that had recycled back to the cell surface. The remaining fluorescence indicated the cell population in which labeled β1 had internalized and had not recycled back to the cell surface.

CDC42 activation assay

HUVEC were seeded at 1×10^6 cells/ml in 100 mm tissue culture dishes (Fisher) in LSGS (5% CO₂, 37°C). On day 3 of plating, cells were treated with DMSO (0.01%) or simvastatin (1.0 μM, 20 h). Cell lysates were harvested on ice, snap-frozen in liquid nitrogen, and the total protein concentration of each lysate adjusted to 12.5 mg/ml for detection of CDC42-GTP using the G-LISA Cdc42 Activation assay (Cytoskeleton, Denver, CO).

Generation of p85 constructs

Site-directed mutagenesis (QuickChange, Agilent Technologies, Santa Clara, CA) of human p85α pCMV6-XL5 (nm_181523.1, Origene, Rockville, MD) was performed to remove the BCR domain. For mutagenesis, the following primer was used: GCAGATGTTGAACAACAAGCTTTGGAATGGAATGAACGACAGCC (corresponding to nucleotides 358–381 and 931–950 of nm_181523.1). The intervening sequence corresponds to the BCR domain of NP_852664 and does not overlap with any other domains. The following

primers were used to amplify p85 Δ BCR in pCMV6-XL5 for topoisomerase cloning into pENTR/D-TOPO (Invitrogen): CACCATGAGTGCTGAGGGG (nucleotides 43–57; nucleotide 43 is the p85 start site in nm_181523.1; 5' CACC added for topoisomerase cloning) and CTATCGCCTCTGCTG (reverse complement of 2214-2203). The cta of the reverse primer added a stop codon. p85 Δ BCR was cloned from pENTR/D-TOPO into pcDNA3.1nV5 using LR Clonase (Invitrogen). p85R274A/pFLAG3 was kindly provided by Dr. Deborah Anderson, Cancer Research Unit, Saskatchewan Cancer Agency, Saskatoon, Saskatchewan. The following primers were used to clone bovine p85R274A from pFLAG3 into pENTR/D-TOPO: CACCATGAGTGCCGAGGGG (nucleotides 1–15 of nm_174575 plus 5' CACC for topoisomerase cloning) and TCGCCTCTGCTGCGCG (reverse complement of 2157-2172), removing the stop codon to fuse at carboxyl terminus with V5 of pcDNA6.2/N-EmGFP. By LR recombination, p85R274A was cloned into pcDNA6.2/N-EmGFP (Invitrogen). Constructs were verified by DNA sequencing and by western blot analysis using anti-V5 (Invitrogen). Control vectors were pcDNA3.1nV5 and pcDNA6.2/N-EmGFP/GW/CAT (Invitrogen).

Transfection

HEK 293A and U-87 MG were seeded at 3×10^5 cells/ml in 35-mm tissue culture dishes (Fisher) and the next day transfected with mutant constructs or vector using FuGENE HD (2 μ g DNA: 6 μ l FuGENE HD). 6 and 20 h post transfection, cells were washed extensively with 1X PBS and media replaced. Assays were performed on day 4 of plating.

S. aureus invasion

ATCC strain #29213 was subcultured daily in tryptic soy broth (200 rpm, 37°C). Bacteria were harvested by centrifugation (10000 rpm, 3 min, 37°C), washed once, and resuspended to 3×10^8 cells/ml in saline. For the invasion assay, transfected cells were washed once with 1X PBS and incubated with the resuspended bacteria (1.2×10^8 cfu/ml, 1 h, 5% CO₂, 37°C). Invasion was terminated by incubation with lysostaphin (20 μ g/ml) and gentamicin (50 μ g/ml) in 10% FBS/PBS (45 min, 5% CO₂, 37°C). Host cells were washed extensively, and suspended using trypsin/EDTA. Trypsin was neutralized by 10% FBS/PBS, cells pelleted (1000 rpm, 3 min) and permeabilized by incubation in 1% saponin/PBS (20 min, 5% CO₂, 37°C). Supernatants containing bacteria were serially diluted into saline and dilutions plated on tryptic soy agar for colony counts (16 h, 37°C). For immunofluorescence, bacteria were harvested as described above and incubated (RT, 10 min) with fibronectin (10 μ g/ml). Following extensive washes with saline, bacteria were added to HUVEC under serum free conditions (1.2×10^8 cfu/ml, 5% CO₂, 37°C) for times indicated.

Statistical analyses

Normally distributed data were analyzed by Student's *t*-test when the comparison was limited to 2 groups or by one-way ANOVA followed by Student-Neuman-Keuls post-hoc analysis when 3 or more groups were compared. Vinculin-containing adhesion complexes and actin structures were evaluated in 100 cells/treatment from randomly selected fields and data assessed using X² test of association (Sigma Stat, Systat, Point Richmond, CA). Differences between groups were considered statistically significant at $p \leq 0.05$.

Results and Discussion

Simvastatin decreases adhesion complex formation

To examine whether the inhibition of *S. aureus* invasion by simvastatin includes disruption of adhesion complexes used by pathogenic strains to gain host cell entry, the effect of simvastatin on the formation of complexes was examined. The formation of adhesion complexes begins with the recruitment of β 1 from the recycling endosome to the plasma membrane [1,2]. Once

localized at the plasma membrane, $\beta 1$ functions as an anchor for the ordered assemblage of components into the complex [3]. The composition of adhesion complexes is cell type and environment dependent, but commonly consists of the signaling molecule phosphoinositide 3-kinase (PI3K) together with cytoskeletal proteins actin, tensin and vinculin which is readily detectable as an elongated structure in fully-formed complexes. In response to DMSO, adhesion complexes were detected in 84% of 3T3-Swiss albino cells whereas in response to simvastatin, complexes were detected in 35% of the cells, a decrease of 49% (Figure 1, $p \leq 0.001$). To examine whether the decrease in adhesion complexes could be due to inhibition of $\beta 1$ recruitment, the response to primaquine, an inhibitor of $\beta 1$ recycling [15], was compared to the effect of simvastatin. Similar to the effect of simvastatin, in response to primaquine, adhesion complexes were detected in fewer cells (59%, Figure 1, $p \leq 0.001$). Decreases were observed in HUVEC as well (DMSO: 84%; simvastatin: 20%; primaquine: 53%, $p \leq 0.001$). These data raised the possibility that simvastatin diminishes the formation of adhesion complexes in part through impaired recycling of $\beta 1$ to the plasma membrane required for the initiation of adhesion complex formation.

Simvastatin inhibits $\beta 1$ uptake and recycling

To investigate directly whether simvastatin exerts an effect on $\beta 1$ trafficking, anti- $\beta 1$ conjugated to Alexa Fluor 488 was tracked within HUVEC in the presence or absence of simvastatin. Surface-labeled $\beta 1$ was more abundant in the population of simvastatin treated cells prior to uptake ($97 \pm 0.1\%$) compared to DMSO treated cells ($92 \pm 0.9\%$, $p \leq 0.001$, Figure 2, Panel A, Pre). Surface-labeled $\beta 1$ remained elevated in the simvastatin treated population following uptake ($97 \pm 0.2\%$ vs. $94 \pm 0.4\%$, $p \leq 0.001$, Figure 2, Panel A, Post). Taken together, these data suggested that simvastatin impairs the uptake of $\beta 1$. To examine whether the increase in cell-surface $\beta 1$ was attributable to increased $\beta 1$ expression rather than to the inhibition of uptake, total $\beta 1$ expression was assessed by western blot analysis of immunoprecipitated $\beta 1$. The integrated intensity values for $\beta 1$ were not different between simvastatin and DMSO treated cells ($p \geq 0.05$), indicating that the increased abundance of cell-surface $\beta 1$ was not associated with an increase in total expression.

To examine further the effect of simvastatin on $\beta 1$ trafficking, the recycling of internalized $\beta 1$ to the cell surface was tracked. Intracellular $\beta 1$ conjugated to Alexa Fluor 488 was detected in $30 \pm 1\%$ of simvastatin treated cells compared to $13 \pm 1\%$ of DMSO treated cells. The greater than 50% difference in internalized, labeled $\beta 1$ that had failed to recycle back to the cell surface indicated that simvastatin impairs $\beta 1$ recycling (Figure 2, Panel B, $p \leq 0.01$). To verify the effectiveness of the removal of antibody from cell-surface $\beta 1$ by acid washing, antibody was allowed to remain intact (– acid wash, Figure 2, Panel C) or subjected to acid washing (+ acid wash, Figure 2, Panel C). Cell-surface anti- $\beta 1$ decreased from $77 \pm 2\%$ of simvastatin treated cells to $0.02 \pm 0.01\%$ with acid treatment. In DMSO treated cells, the decrease was from $72 \pm 8\%$ to $0.3 \pm 0.02\%$ ($p \leq 0.001$), indicating that regardless of treatment, acid washing removes cell-surface anti- $\beta 1$. Taken together, simvastatin exerts an effect on adhesion complexes by both restricting the uptake of complexes that already had formed and by disrupting their nascent formation through inhibition of $\beta 1$ recycling to the plasma membrane.

Simvastatin could exert dual effects on $\beta 1$ through multiple prenylation-dependent proteins. We next focused on CDC42 as this small-GTPase functions upstream of Rac in the formation of vinculin-containing adhesions [16], independently of Rac in recycling [17], and within membrane compartments during host invasion [6].

S. aureus invasion as well as simvastatin pre-treatment stimulate CDC42 activation

Filopodia formation, indicative of CDC42 activation, was observed more frequently in infected cells (56%) compared to uninfected cells (9%, Figure 3, Panel A, $p \leq 0.001$). Filopodia

formation likewise was more frequent in simvastatin treated cells compared to DMSO treated cells (89% vs. 6%, $p \leq 0.001$, Figure 3, Panel B). To confirm CDC42 activation, GTP-loading was examined. Simvastatin stimulated GTP-loading of CDC42 1.4 \pm 0.06 fold over DMSO control ($p \leq 0.05$, Figure 3, Panel C).

These findings revealed an apparent contradiction in that simvastatin stimulated CDC42 activation yet diminished adhesion complexes that are dependent upon CDC42 activation early in their formation. From this, we explored the possibility that simvastatin inhibition is through cytosolic sequestration of activated CDC42 rather than through inhibition of CDC42 activation. As both timing and localization of GTPase inactivation appear to be critical for appropriate trafficking of vesicles from the plasma membrane to the lysosomal or recycling compartments [14], we investigated the potential role of the GAP protein p85 that binds preferentially to activated CDC42 [18] and is sequestered within the cytosol, coupled to CDC42, in response to simvastatin.

Similar to the effect of simvastatin, loss of p85 GAP activity decreases host cell invasion and β 1 trafficking

S. aureus invasion was diminished to 36 \pm 9% of control values ($p \leq 0.001$) in host cells expressing a mutated form of p85 in which the arginine residue at position 274 required for GAP activity was substituted with alanine (p85R274A; Figure 4, Panel A). Expression of a deletion mutant in which the BCR homology domain required for coupling to CDC42 decreased host invasion to 64 \pm 4% of control ($p \leq 0.001$).

To examine whether the decrease in invasion might be associated with impaired regulation by p85 over trafficking of the β 1 receptor, fluorescently-labeled β 1 was tracked within cells expressing p85R274A. 23 \pm 0.6% of host cells expressing p85R274A retained intracellular β 1 compared to 15 \pm 0.2% of control cells. The intracellular retention by p85R274A expressing cells exceeds that of control cells by 35% ($p \leq 0.001$), indicating that loss of p85 GAP activity inhibits β 1 recycling (Figure 4, Panel B). Cell surface β 1 was detected on more cells expressing p85R274A (75 \pm 1%) than control (69 \pm 0.2%, $p \leq 0.05$), suggesting that loss of p85 GAP activity restricts β 1 uptake (Figure 4, Panel C). Our findings reveal that loss of p85 GAP activity inhibits host cell invasion and the uptake and recycling of β 1 in a manner similar to the inhibition by simvastatin. From these findings, we propose a mechanism whereby membrane-localized p85 GAP activity facilitates uptake and recycling of the β 1 receptor and that the mechanism of inhibition by simvastatin of host invasion includes the cytosolic sequestration of p85.

Abbreviations

GTPases	small-guanosine triphosphatases
PI3K	phosphoinositide 3-kinase
HMG-CoA	3-hydroxy-3-methylglutaryl coenzyme A
GAP	GTPase activating protein
BCR	breakpoint cluster region

Acknowledgments

The authors thank Dr. Deborah Anderson, Ph.D., Cancer Research Unit Saskatchewan Cancer Agency, Saskatoon, Saskatchewan, for her generous gift of p85R274A/pFLAG3 and Dr. Chris Vlahos, Eli Lilly & Co., for guidance throughout this project. This work was funded by the National Institutes of Health National Heart, Lung and Blood Institute [Grant 1R15HL092504].

References

1. Bretscher MS. Endocytosis and recycling of the fibronectin receptor in CHO cells. *Embo J* 1989;8:1341–1348. [PubMed: 2527741]
2. Powelka AM, Sun J, Li J, et al. Stimulation-dependent recycling of integrin beta1 regulated by ARF6 and Rab11. *Traffic* 2004;5:20–36. [PubMed: 14675422]
3. Miyamoto S, Teramoto H, Coso OA, et al. Integrin function: molecular hierarchies of cytoskeletal and signaling molecules. *J Cell Biol* 1995;131:791–805. [PubMed: 7593197]
4. Hauck CR, Ohlsen K. Sticky connections: extracellular matrix protein recognition and integrin-mediated cellular invasion by *Staphylococcus aureus*. *Curr Opin Microbiol* 2006;9:5–11. [PubMed: 16406780]
5. Garzoni C, Kelley WL. *Staphylococcus aureus*: new evidence for intracellular persistence. *Trends Microbiol* 2009;17:59–65. [PubMed: 19208480]
6. Horn MP, Knecht SM, Rushing FL, et al. Simvastatin inhibits *Staphylococcus aureus* host cell invasion through modulation of isoprenoid intermediates. *J Pharmacol Exp Ther* 2008;326:135–143. [PubMed: 18388257]
7. Merx MW, Liehn EA, Janssens U, et al. HMG-CoA reductase inhibitor simvastatin profoundly improves survival in a murine model of sepsis. *Circulation* 2004;109:2560–2565. [PubMed: 15123521]
8. Terblanche M, Almog Y, Rosenson RS, et al. Statins and sepsis: multiple modifications at multiple levels. *Lancet Infect Dis* 2007;7:358–368. [PubMed: 17448939]
9. Donnino MW, Cocchi MN, Howell M, et al. Statin therapy is associated with decreased mortality in patients with infection. *Acad Emerg Med* 2009;16:230–234. [PubMed: 19281494]
10. Dobesh PP, Klepser DG, McGuire TR, et al. Reduction in mortality associated with statin therapy in patients with severe sepsis. *Pharmacotherapy* 2009;29:621–630. [PubMed: 19476415]
11. Endo A. The discovery and development of HMG-CoA reductase inhibitors. 1992. *Atheroscler Suppl* 2004;5:67–80. [PubMed: 15531278]
12. Sinensky M. Recent advances in the study of prenylated proteins. *Biochim Biophys Acta* 2000;1484:93–106. [PubMed: 10760460]
13. Chamberlain MD, Berry TR, Pastor MC, et al. The p85alpha subunit of phosphatidylinositol 3'-kinase binds to and stimulates the GTPase activity of Rab proteins. *J Biol Chem* 2004;279:48607–48614. [PubMed: 15377662]
14. Rodman JS, Wandinger-Ness A. Rab GTPases coordinate endocytosis. *J Cell Sci* 2000;113:183–192. [PubMed: 10633070]
15. Bretscher MS. Circulating integrins: alpha 5 beta 1, alpha 6 beta 4 and Mac-1, but not alpha 3 beta 1, alpha 4 beta 1 or LFA-1. *Embo J* 1992;11:405–410. [PubMed: 1531629]
16. Nobes CD, Hall A. Rho, rac, and cdc42 GTPases regulate the assembly of multimolecular focal complexes associated with actin stress fibers, lamellipodia, and filopodia. *Cell* 1995;81:53–62. [PubMed: 7536630]
17. Sabharanjak S, Sharma P, Parton RG, et al. GPI-anchored proteins are delivered to recycling endosomes via a distinct cdc42-regulated, clathrin-independent pinocytic pathway. *Dev Cell* 2002;2:411–423. [PubMed: 11970892]
18. Zheng Y, Bagrodia S, Cerione RA. Activation of phosphoinositide 3-kinase activity by Cdc42Hs binding to p85. *J Biol Chem* 1994;269:18727–18730. [PubMed: 8034624]

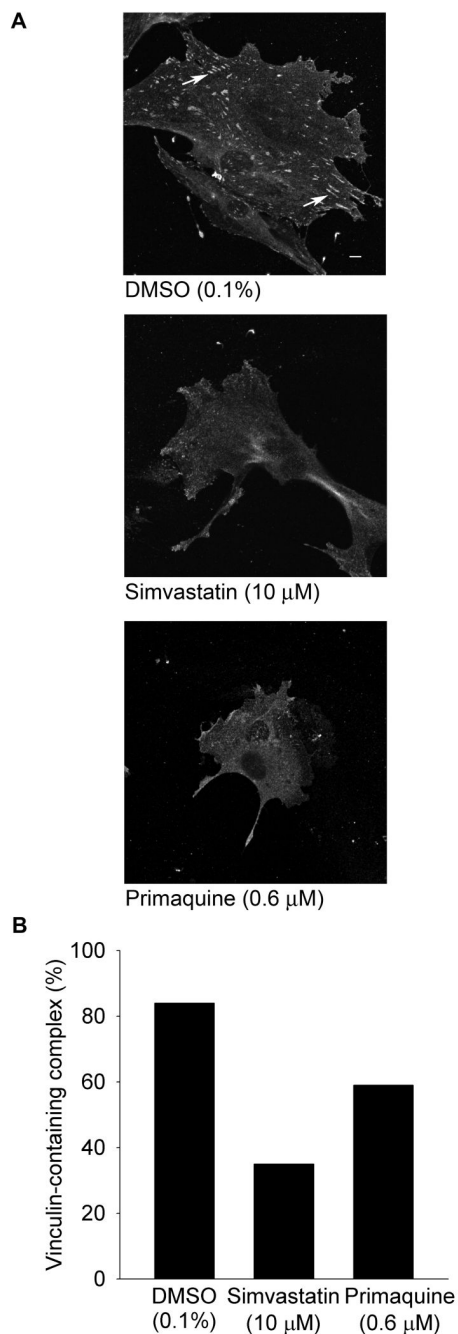
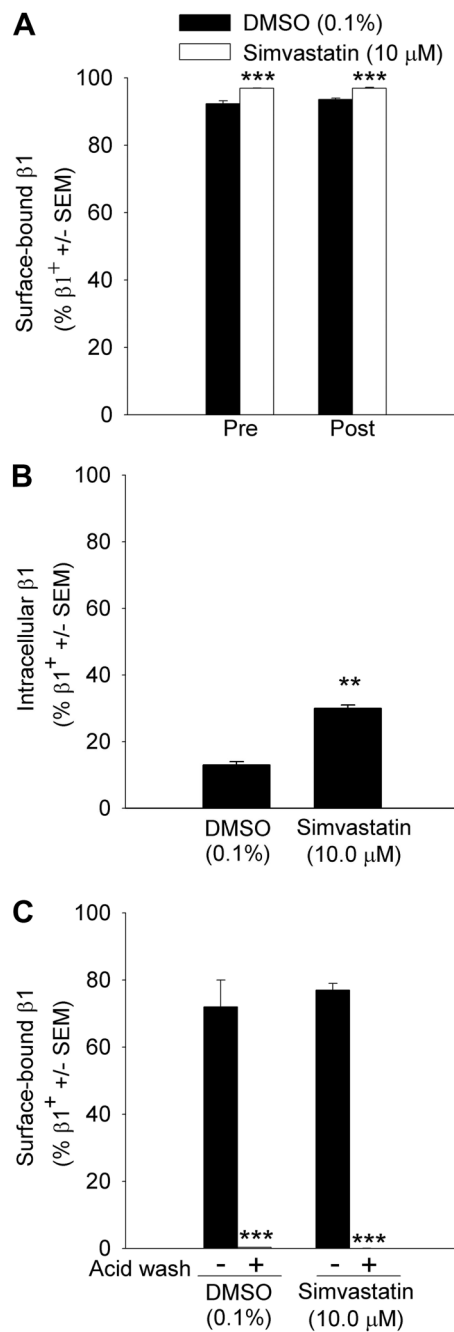


Figure 1.

Inhibition of recycling by primaquine decreases vinculin-containing adhesion complexes.

Panel A 3T3-Swiss albino cells were pre-treated with dimethyl sulfoxide (DMSO, 0.1%) in the presence of simvastatin (10 μ M), or of primaquine (0.6 μ M, 20 h, 37°C, 5% CO₂), fixed, permeabilized, blocked, and stained with anti-vinculin followed by anti-mouse Alexa Fluor 488. Arrows indicate vinculin-containing complexes. Scale bar is 10 μ m. **Panel B** Data presented as the percentage of cells displaying vinculin-containing adhesion complexes. 100 cells/treatment from randomly selected fields were evaluated ($p \leq 0.001$ by X² test of association).

**Figure 2.**

Simvastatin inhibits $\beta 1$ trafficking **Panel A** Human umbilical vein endothelial cells (HUVEC) were pretreated with dimethyl sulfoxide (DMSO, 0.1%) or simvastatin (10 μ M, 20 h, 37°C, 5% CO₂), and cell-surface $\beta 1$ examined prior to the stimulation of endocytosis (Pre) or after the stimulation of endocytosis (Post). Data are representative of replicate experiments, n = 2–3/treatment (***)greater than DMSO, $p \leq 0.001$, one-way ANOVA followed by Student-Neuman-Keuls post-hoc analysis). **Panel B** *Simvastatin decreases recycling of $\beta 1$ to the cell surface.* To enable uptake and recycling of fluorescently-labeled $\beta 1$, HUVEC were pretreated as described in Panel A followed by the labeling of cell-surface $\beta 1$ with anti- $\beta 1$ conjugated to Alexa Fluor 488 (4°C, 1 h). Uptake and recycling then were initiated in pre-labeled cells by

incubation at 37°C for 120 min. To remove Alexa Fluor-conjugated antibody bound to $\beta 1$ that had remained at the cell surface or from $\beta 1$ that had recycled back to the cell surface, acid washes were performed. Fluorescence following the acid wash treatment indicated labeled $\beta 1$ that had internalized and had failed to recycle to the cell surface. Data are representative of replicate experiments, $n = 2/\text{treatment}$ (**greater than DMSO, $p \leq 0.01$, Student's t -test). **Panel C Acid wash removes cell-surface anti- $\beta 1$.** To verify the effectiveness of acid washing in the removal of cell-surface anti- $\beta 1$ regardless of treatment, HUVEC were pre-treated as in Panel A. Cell-surface $\beta 1$ was fluorescently labeled by incubating cells with anti- $\beta 1$ conjugated to Alexa Fluor 488 (4°C, 1 h). Surface-bound antibody was allowed to remain intact (– acid wash) or was removed by cold acid washes (+ acid wash; ***less than non-acid wash, $p \leq 0.001$, one-way ANOVA followed by Student-Neuman-Keuls post-hoc analysis, $n = 2/\text{treatment}$).

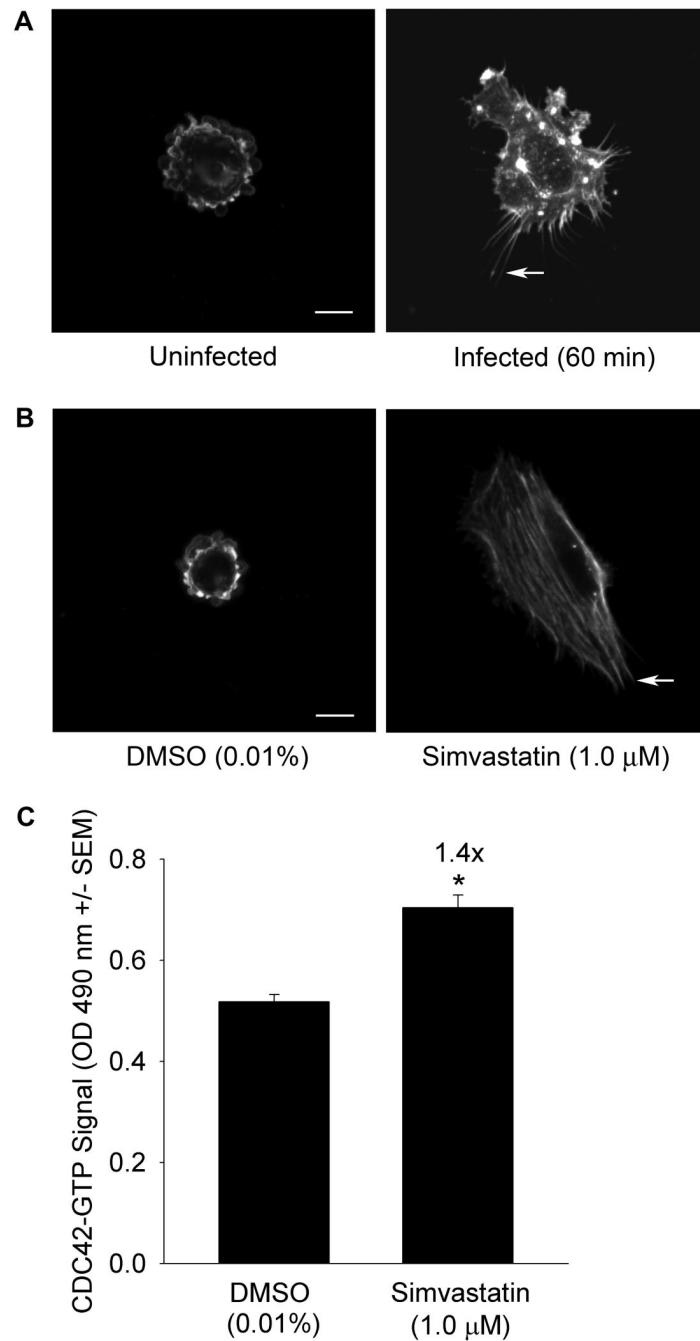
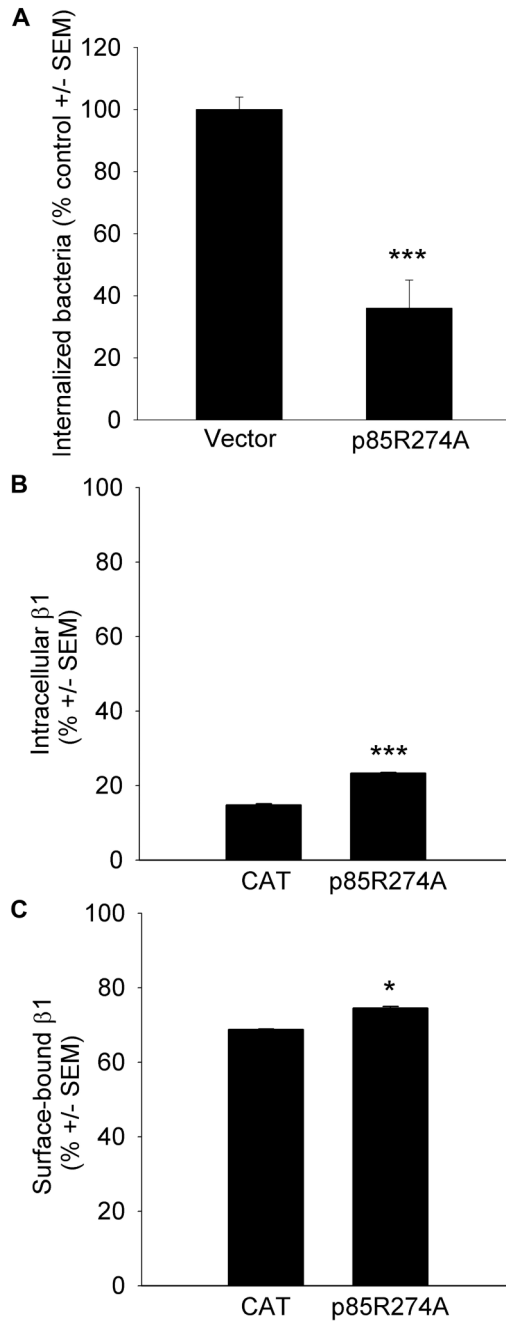


Figure 3.

Panel A *S. aureus* invasion stimulates filopodia formation. Human umbilical vein endothelial cells (HUVEC) were serum starved (20 h) then infected with *S. aureus* that had been pre-incubated with fibronectin (60 min, 37°C, 5% CO₂). Cells were fixed, permeabilized, blocked, and actin detected using Alexa Fluor 488 phalloidin. Arrows indicate representative filopodia. Size bar: 10 μm. Induction was scored in 100 cells/treatment from randomly selected fields. Filopodia formation was greater in infected cells (56%) than in uninfected cells (9%, $p \leq 0.001$ by X² test of association). Data and images are representative of replicate experiments. **Panel B** *Simvastatin* stimulates filopodia formation. HUVEC were serum starved in the presence of dimethyl sulfoxide (DMSO, 0.01%) or simvastatin (1.0 μM, 20 h, 37°C, 5% CO₂). Filopodia

were detected and quantified as in Panel A. Filopodia formation was more frequent in simvastatin treated cells (89%) compared to DMSO treated cells (6%, $p \leq 0.001$ by X^2 test of association). **Panel C** *Simvastatin stimulates GTP-loading of CDC42*. HUVEC were treated as in Panel B and GTP-bound CDC42, indicated by absorbance at 490 nm, measured by G-LISA. Data are representative of replicate experiments with $n = 4/\text{treatment}$ (*significantly greater than DMSO, Student's t -test, $p \leq 0.05$).

**Figure 4.**

Similar to the effect of simvastatin, loss of p85 GAP activity decreases host cell invasion and $\beta 1$ trafficking. **Panel A** Host cell invasion by *S. aureus* was assessed in human embryonic kidney (HEK) 293A cells transiently transfected with p85R274A, a mutated form of p85 in which the arginine within the breakpoint cluster region (BCR) homology domain required for GAP activity has been substituted with an alanine or in control cells transfected with pcDNA5. 48 h post transfection, host cell invasion by *S. aureus* was initiated (1 h, 37°C, 5% CO₂), followed by the removal of extracellular bacteria using the bactericides lysostaphin and gentamicin. Intracellular bacteria were released using the detergent saponin and colony counts from serial dilutions of the media performed. Data are colony counts shown as % control

± SEM and are representative of replicate experiments, n = 5/construct (***)less than control, $p \leq 0.001$ by Student's *t*-test). **Panel B** *β1 recycling is diminished in p85R274A/NEmGFP expressing cells* U-87 MG were transiently transfected with p85R274A/N-EmGFP or with the control expression vector chloramphenicol acetyl transferase (CAT) /N-EmGFP. 20 h prior to analysis, cells were serum starved. Cell surface β1 was fluorescently labeled by incubating cells with anti-β1 conjugated to Alexa Fluor 555 at 4°C. Following uptake and recycling of the fluorescently-labeled β1 by incubating cells at 37°C (1 h), antibody bound to β1 that had remained at the cell surface or that had recycled back to the cell surface was removed by acid washes. Fluorescence at 555 in GFP+ cells following the acid wash was indicative of intracellular, labeled β1 that had internalized but had not recycled back to the cell surface in the transfected population (***)greater than CAT/N-EmGFP, $p \leq 0.001$, Student's *t*-test, n = 3/construct). **Panel C** *β1 uptake is diminished in p85R274A/N-EmGFP expressing cells*. To assess cell-surface β1 in transfected cells, uptake was stimulated in unlabeled cells by incubating at 37°C for 60 min followed by surface labeling with anti-β1 conjugated to Alexa Fluor 555. Fluorescence at 555 in GFP+ cells indicated cell-surface β1 in the transfected population (*greater than CAT/N-EmGFP, $p \leq 0.05$, Student's *t*-test, n = 2/construct).